Journal of Nuclear Materials 438 (2013) S422–S425

Contents lists available at SciVerse ScienceDirect

Journal of Nuclear Materials

journal homepage: www.elsevier.com/locate/jnucmat

Heat transfer of TEMHD driven lithium flow in stainless steel trenches

W. Xu, D. Curreli, D. Andruczyk, T. Mui, R. Switts, D.N. Ruzic *,1

Center for Plasma–Material Interactions, Department of Nuclear, Plasma and Radiological Engineering, University of Illinois at Urbana–Champaign, 104 S. Wright St., Urbana, IL 61801, USA

ARTICLE INFO

Article history:
Available online 12 January 2013

ABSTRACT

The Lithium/Metal Infused Trenches (LiMITs) concept, which utilizes the thermoelectric magnetohydrodynamic (TEMHD) driven flowing liquid lithium to cool the divertor surface, has been successfully demonstrated at the University of Illinois. The IR camera results show that such self-driven flowing liquid lithium in the open surface stainless steel trench structure can withstand heat fluxes of up to 10 MW/m^2 for 10 s without significant evaporation. A clear asymmetric temperature distribution was observed from the IR result and such asymmetry can be affected by the direction of the driven magnetic field. Thermocouples are embedded in different positions to monitor the temperature within the lithium. These direct measurements also reveal that flowing liquid lithium can effectively bring the heat from the direct heating area and the efficiency can be influenced by magnetic field and heating power.

1. Introduction

Heat transfer of the plasma facing component (PFC) is one of the key challenges for first wall research. With the increasing power needed for fusion reactors, traditional solid materials start to suffer from the intense sputtering and thermal stress which may eventually lead to the failure of the PFC. An alternative is to use flowing liquid metal such as liquid lithium, Sn–Li compounds, and gallium [1,2]. The liquid metal flow and heat transfer related to fusion reactor have been studied for years and the potential of using flowing liquid metal is significant [3].

Using free liquid lithium for divertor was firstly raised at University of Wisconsin [4]. Gallium film was firstly used as the limiter and later the divertor on T-3M [5,6]. Because of the difficulty to flow liquid metal in strong magnetic field many methods have been considered such as liquid metal film, liquid metal jets, and liquid metal droplets [7]. A big disadvantage of the above free-surface flow methods is that liquid metal might ejects into plasma due to the incoming current from the plasma [8]. Possible solutions include grounding along the toroidal direction [9] and capillary porous system (CPS) [10].

Among all possible candidate materials lithium has drawn a lot of interest since the lithium injection experiment on TFTR showed a significant improvement of the plasma performance [11]. The passive pumping of hydrogen isotopes by liquid lithium surface provides the ability of achieving low recycling wall [12,13]. During open lithium surface experiment on CDX-U it was occasionally discovered that a thin pool of liquid lithium can withstand 60 MW/m^2 of electron beam heating without significant evaporation and liquid lithium can swirl by itself [14]. More experiments and analysis [15] revealed that this is due to the thermoelectric magnetohydrodynamic (TEMHD) driven flow, originally discussed in 1979 by Shercliff [16]. Based on this effect a new concept, the Lithium–Metal Infused Trenches (LiMIT), which drives liquid lithium flow in open-surface metal trenches was envisioned and proven feasible at the University of Illinois [17]. Liquid lithium was observed to flow inside the trench at the speed of 0.22 ± 0.03 m/s. A one dimensional model was developed to describe the flow inside the structure [17]. In this paper the detailed heat transfer of this concept will be discussed to reveal its potential application for fusion reactors.

2. Experiment design and setup

The thermoelectric effect is the key of LiMIT concept. When a temperature gradient exists, charge carriers tend to diffuse more along the temperature gradient and, just like in thermocouples, such diffusion can drive thermoelectric current inside heated liquid metal. In experiment this thermoelectric current is affected by an external magnetic field to drive the liquid lithium flow along stainless steel trenches.

The experiment setup is shown in Fig. 1. The purpose of LiMIT is to build a self-driven flow in magnetic field to remove the severe heat flux of fusion reactor while presenting a fresh lithium surface to the plasma. In our experiment, a linear electron beam with Gaussian distribution generating heat fluxes <10 MW/m^2 is used

* Corresponding author.
E-mail address: druzic@illinois.edu (D.N. Ruzic).
[1] Presenting author

0022-3115/$ - see front matter © 2013 Elsevier B.V. All rights reserved.
http://dx.doi.org/10.1016/j.jnucmat.2013.01.085

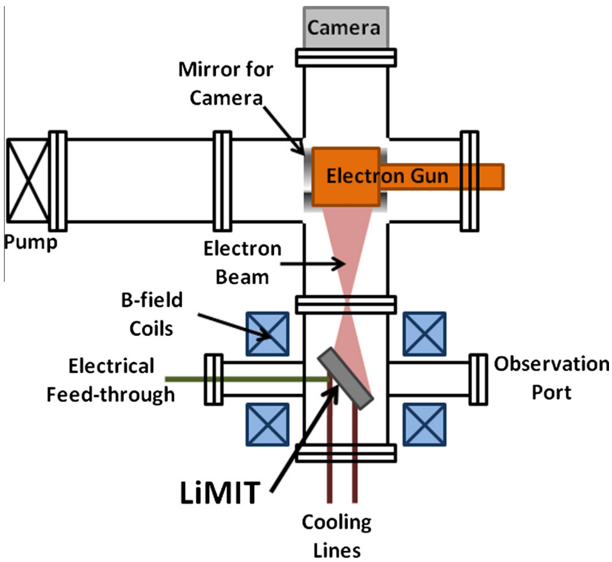

Fig. 1. Experiment setup for the TEMHD driven lithium–metal infused trench flow experiment.

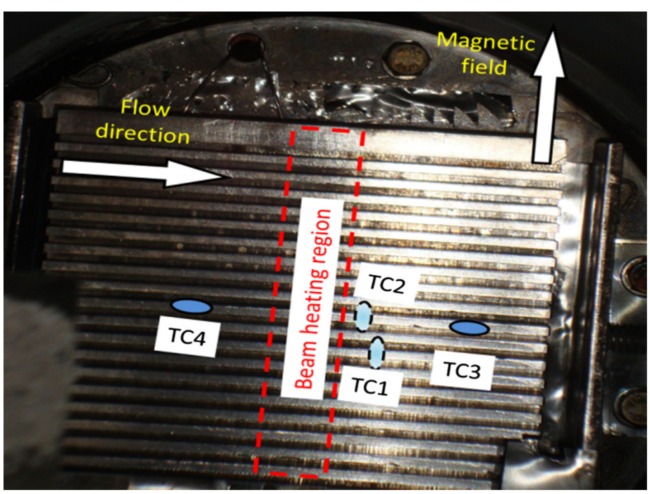

Fig. 2a. Top view of the trench with stainless steel tray.

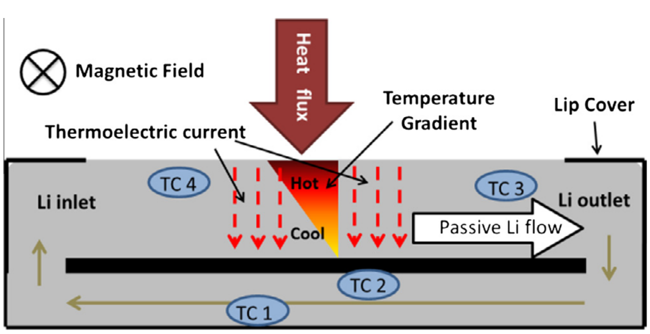

Fig. 2b. Cross section view of the tray design. Four thermocouples (TC1–TC4) are embedded. TC3 and TC4 are embedded in the trench. TC1 is attached to the bottom inner face of the tray. TC2 is attached to the back side of the trench structure.

to mimic the high heat flux in the divertor. A Helmholtz coil is used to generate a magnetic field parallel with the electron beam which ranges from zero to about 800 Gauss.

The lithium tray is tilted by 60° relative to the floor so the angle between the beam and the tray is about 30°. Liquid lithium does not fall out of the trench because of the surface tension. An infrared camera (Inframetrics 760) is used to monitor the surface temperature change of the trench.

The lithium tray has 2 mm wide and 1 cm deep stainless steel trenches built on the top side and a gap at bottom side for return flow which form a closed loop. The top surface is heated by the electron beam while the bottom surface is actively cooled. Four thermocouples (TC1–TC4) are embedded inside lithium (see Figs. 2a and 2b). TC4 is placed closer to the direct heating area than TC3 and the reason will be discussed in detail.

3. Results

3.1. IR camera measurement

The IR camera is observing the lithium surface through a ZnSe viewport. Since the emissivity of liquid lithium is very low, the IR measurement becomes sensitive to the emissivity calibration. Previous in situ calibration found that the emissivity of liquid lithium between 200 °C and 300 °C is about 0.046 and the wavelength range of the IR camera is 8–12 μm [18]. The IR measurement can be disturbed by the IR emission from the impurity scale on the surface which looks like a hot spot in the IR image and the reflection of IR light from the beam filament. Without the acceleration voltage one IR image was taken when the filament is heated to the required temperature as a background image. After IR measurement was taken in experiments the subtraction of both images gives the actual temperature rise caused by heating.

Fig. 3 is the temperature increase when the tray was heated by a 3 MW/m^2 beam for about 20 s and the transverse magnetic field is 589 Gauss. In the IR image lithium trenches look like cooler thin stripes lying horizontally and the hotter region is mostly stainless steel wall and impurity since their emissivity is higher. Some cold spots in the hot region are caused by the subtraction of the saturation regions. The asymmetric temperature distribution is clearly shown in the figure. It is predicted that lithium flows from right to left and Fig. 3 shows that such flow can bring the heat away from the center region to the left side while the right side has much smaller temperature increase. At the position where lithium meets the electron beam the steep temperature gradient can be observed.

When the magnetic field is changed to the opposite direction, the liquid metal is expected to invert its flow. This is confirmed by our experiment, where an asymmetry of the temperature distribution is found after the reversal of the field, as reported in Fig. 4.

3.2. Thermocouple results

Fig. 5 shows the temperature change of embedded thermocouples when lithium was heated from solid to liquid. Because TC4 is placed closer to the heating area, its temperature increases faster than TC3 and the temperature difference keeps increasing. After the lithium starts to melt TC4 does not increase while TC3 increases to the melting point. After the lithium is totally melted the flow starts to build up which brings cooler lithium towards the heating area and transfers heat from the heated area to the downstream side so that the subtraction of (TC3–TC4) quickly becomes a positive value, which is also proved by the IR image. This flow also increases the heat transfer to the back flow channel and this explains the speedup of the TC1 temperature increase after the top trench is totally melted (at $t \sim 40$ s).

Previous swirling flow experiment [15] found that TEMHD driven flow can exist for a long time after the direct heating is turned off while the magnetic field still exists. Such effect also appears in

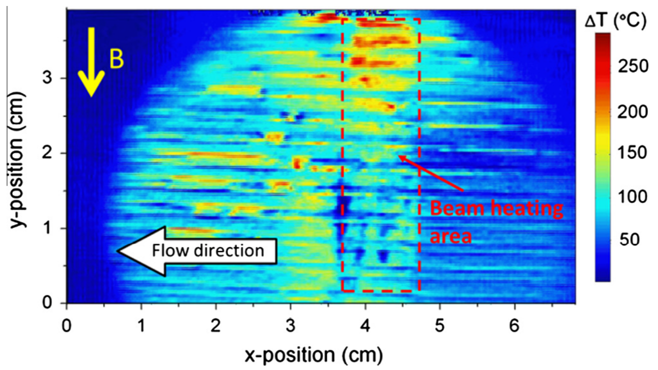

Fig. 3. Surface IR temperature contour of liquid lithium when the center is directly heated [17].

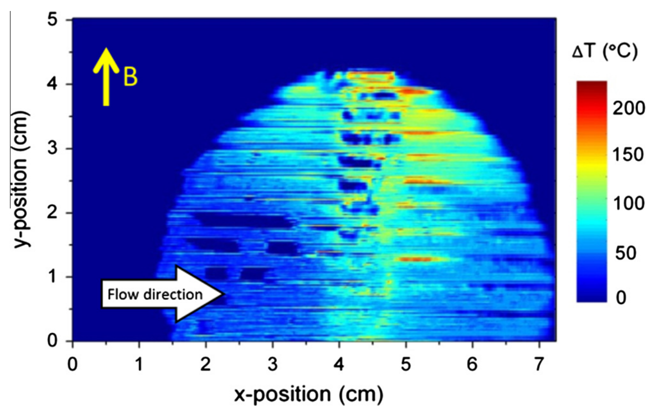

Fig. 4. Surface temperature contour of liquid lithium after the magnetic field is changed to the opposite direction.

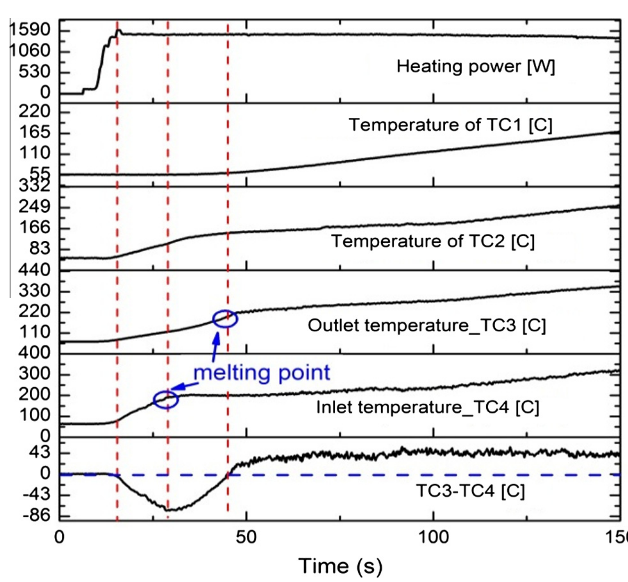

Fig. 5. Temperature changes of embedded thermocouples when lithium is heated from solid to liquid phase.

the trench flow, as is shown in Fig. 6. After the heating is turned off the inlet temperature will stay at a high value for about 3.1 s before it starts to decrease. If the magnetic field is turned off when the heating stops the temperature of the outlet will immediately decrease. In addition with the magnetic field the speed of the falling

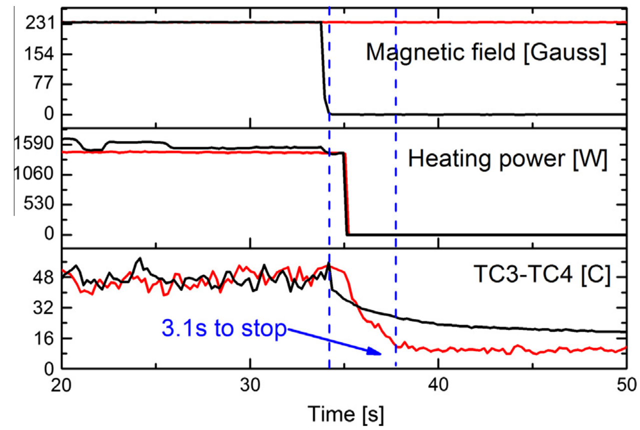

Fig. 6. Comparison of the temperature changes of thermocouples inside the lithium trench when the magnetic field is kept on or off after the electron beam is turned off.

temperature difference between TC3 and TC4 quickly decreases to a low value since the continuous flow acts to even-out the temperature profile along the trench.

A simple 1D model built in the previous work [17] reveals that a higher heating power can lead to a higher temperature gradient which will in turn accelerate the fluid and mitigate the temperature gradient. The overall effect is the relation between the temperature increase and the heating power is less than linear. This is also observed in Fig. 7a. After the beam is turned on, the temperature difference between inlet and outlet starts to ramp up, but after few seconds (<5 s) it becomes stable since the fluid has already been accelerated to a stable velocity and during the 30 s heating pulse the temperature difference keeps more or less stable. From 1 kW to 3 kW the temperature difference only increases by a factor of two.

The 1D model also predicts that as a function of the magnetic field the temperature difference decreases to a minimum point and then increases. According to our calculation within the experiment parameter range the temperature difference should increase when the magnetic field increases. But in Fig. 7b the temperature difference seems decreases when magnetic field increases. More experiments need to be done to explore this effect on a larger magnetic field range.

4. Discussion of the heat transfer

From the IR contour the intensity values along the trenches (totally 10 trenches are chosen) are measured and scaled to the temperature. This process gives the average temperature increase along the lithium trench of 28.3 ± 9.8 °C across the heating area. The comparably large error may come from the influence of the surface impurities. From previous experiments it was discovered that when the heating power is 1500 W and the transverse magnetic field is 589 Gauss the flow velocity is 0.22 ± 0.03 m/s by particle image velocimetry (PIV) [17] which gives a Peclet number of about 43 so that the convection heat transfer should dominate. Assuming that the energy absorbed by the trench is all transferred out by the flow and assuming a linear temperature change from the top to the bottom of the trench, the average flow velocity can be roughly estimated by $\bar{u} = \frac{q}{\rho C_p h w \frac{\Delta T}{2}}$, where q is the power absorbed by the trench (75 W), ρ is the density, C_p is the heat capacity, h is the height of the trench (1 cm) and w is the width of the trench (0.2 cm). The calculated velocity is 0.12 ± 0.04 m/s and this differs from the velocity measured in experiment almost by a factor of two.

The influence from the beam current is not the reason for the big difference. The current from the beam is 150 mA and it is deposited onto a 7 cm by 0.7 cm rectangular area which leads to about 300 A/

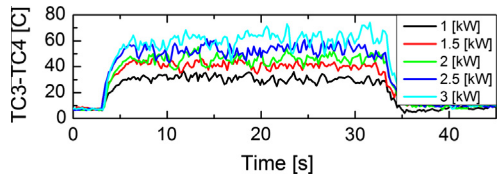

Fig. 7a. Temperature differences between inlet and outlet of a lithium trench with different power.

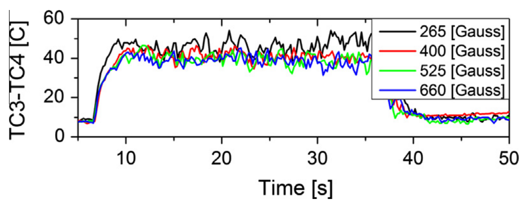

Fig. 7b. Temperature differences between inlet and outlet of a lithium trench in different magnetic fields.

Table 1
Heat transfer of the trench flow through conduction and convection.

Total power (W)	Conduction heat transfer (W)	Convection heat transfer (W)
1056	494 (47%)	526 (53%)
1655	651 (39%)	1003 (61%)
1928	729 (38%)	1199 (62%)
2418	842 (35%)	1575 (65%)
2963	972 (33%)	1991 (67%)

m^2 current density while the thermoelectric current density estimated as $S\sigma(\partial T/\partial z)$ is 1.75×10^5 A/m^2. The induced MHD current is of the same level as the thermoelectric current. So the current from the electron beam can be safely neglected.

However some initial 3D fluid simulation reveals that such flow seems to have a fast top layer while most part of the fluid stays at a comparably lower velocity. In the region close to heated stainless steel wall the flow velocity will speed up to increase the local heat transfer rate which makes the assumption for the energy balance not completely valid.

Due to the flow in the long and narrow duct, little amount of lithium flows from top surface to the bottom of the trench and in this case the Peclet number on the direction from top to bottom is small. The heat transfer inside the trench should include conduction from top to bottom and convection along the trench. If the temperature of the bottom inside the trench is assumed to be the same as the inlet then in Fig. 7a, then the conduction heat transfer can be easily calculated with the measured temperature difference. The convection heat transfer can be calculated by the subtraction from the total absorbed power. Table 1 shows the portion of conduction and convection of which the convection part is larger when the total power becomes higher.

5. Conclusion

In this paper the heat transfer of the TEMHD driven open duct flow is investigated. With an IR camera and embedded thermocouples the unique temperature variation in response to surface heating and magnetic field is measured and analyzed under different experiment conditions. Heat transfer analysis reveals that LiMIT concept has the ability to achieve surface heat flux mitigation, convection cooling and passive pumping of liquid lithium in a low magnetic field and may be extendable to higher fields as well. Future work will include a complete 3D heat transfer and fluid flow model that can describe the detail of the fluid field, as well as experimental validation at higher magnetic fields. The MHD effect on the heat transfer, especially the cooling of the wall in the direct heating region, would be an important topic for the application in real fusion reactors.

Acknowledgments

The authors would like to thank Dr. Dennis Youchison from Sandia National Lab for helping us build up the IR system, Guizhong Zuo from Institute of Plasma Physics, Chinese Academy of Science and Dr. Mike Jaworski from Princeton Plasma Physics Lab for many fruitful discussions. This work is supported under DOE Contracts DE-FG02-99ER54515.

References

[1] M. Greenwald, R. Callis, D. Gates, B. Dorland, J. Harris, R. Linford, M. Mauel, K. McCarthy, D. Meade, F. Najmabadi, B. Nevins, J. Sarff, M. Ulrickson, M. Zarnstorff, S. Zinkle, Tech. Rep., Fusion Energy Science Advisory Committee 2006.
[2] M.A. Abdou, Fusion Engineering and Design 54 (2001) 181.
[3] N. Morley, S. Smolentsev, L. Barleon, I.R. Kirillov, M. Takahashi, Fusion Engineering and Design 51 (2000) 701.
[4] B. Badger, M.A. Abdou, R.W. Boom, R.G. Brown, E.T. Cheng, R.W. Conn, J.M. Donhowe, L.A. El-Guebaly, G.A. Emmert, G.R. Hopkins, W.A. Houlberg, A.B. Johnson, J.H. Kamperschroer, D. Klein, G.L. Kulcinski, R.G. Lott, D.G. McAlees, C.W. Maynard, A.T. Mense, G.R. Neil, E. Normand, P.A. Sanger, W.E. Stewart, T. Sung, I.N. Sviatoslavsky, D.K. Sze, W.F. Vogelsang, L.J. Wittenberg, T.F. Yang, W.D. Young, UWFDM-68 1974.
[5] V.O. Vodyanyuk, V.N. Dem'yanenko, A.F. Kolesnichenko, et al., Fizika Plasmi (Russian) 14 (1988) 628–632.
[6] S.V. Mirnov, V.N. Dem'yanenko, E.V. Murav'ev, Journal of Nuclear Materials 196–198 (1992) 45–49.
[7] S. Molokov, Technical Report ANL/TD/TM99-08, Argonne National Lab 1999.
[8] D.G. Whyte, T.E. Evans, C.P.C. Wong, W.P. West, R. Bastasz, J.P. Allain, J.N. Brooks, Fusion Engineering and Design 72 (2004) 133–147.
[9] R. Majeski, S. Jardin, R. Kaita, T. Gray, P. Marfuta, J. Spaleta, J. Timberlake, L. Zakharov, G. Antar, R. Doerner, S. Luckhardt, R. Seraydarian, V. Soukhanovski, R. Maingi, M. Finkenthal, D. Stutman, D. Rodgers, S. Angelin, Nuclear Fusion 45 (2005) 519.
[10] V.A. Evtikhin, I.E. Lyublinski, A.V. Vertkov, S.V. Mirnov, V.B. Lazarev, Fusion Engineering and Design 56–57 (2001) 363–367.
[11] D.K. Mansfield, D.W. Johnson, B. Grek, H.W. Kugel, M.G. Bell, R.E. Bell, R.V. Budny, C.E. Bush, E.D. Fredrickson, K.W. Hill, D.L. Jassby, R.J. Maqueda, H.K. Park, A.T. Ramsey, E.J. Synakowski, G. Taylor, G.A. Wurden, Nuclear Fusion 41 (2001) 1823.
[12] M. Nieto, D.N. Ruzic, W. Olczak, R. Stubbers, Journal of Nuclear Materials 350 (2006) 101–112.
[13] D.N. Ruzic, M. Nieto, J.P. Allain, M.D. Coventry, Journal of Nuclear Materials 313–316 (2003) 646–650.
[14] R. Kaita, R. Majeski, T. Gray, H. Kugel, D. Mansfield, J. Spaleta, J. Timberlake, L. Zakharov, R. Doerner, T. Lynch, R. Maingi, V. Soukhanovskii, Physics of Plasmas 14 (2007) 056111.
[15] M.A. Jaworski, T.K. Gray, M. Antonelli, J.J. Kim, C.Y. Lau, M.B. Lee, M.J. Neumann, W. Xu, D.N. Ruzic, Physical Review Letters 104 (2010) 094503.
[16] J.A. Shercliff, Journal of Fluid Mechanics 91 (1979) 231.
[17] D.N. Ruzic, W. Xu, D. Andruczyk, M.A. Jaworski, Nuclear Fusion 51 (2011) 102002.
[18] W. Xu, V. Surla, M.A. Jaworski, M. Lee, T. Mui, M.J. Neumann, D.N. Ruzic, Journal of Nuclear Materials 415 (2011) 981.